

N72-33836

MSC-04112  
SUPPLEMENT 8



NATIONAL AERONAUTICS AND SPACE ADMINISTRATION

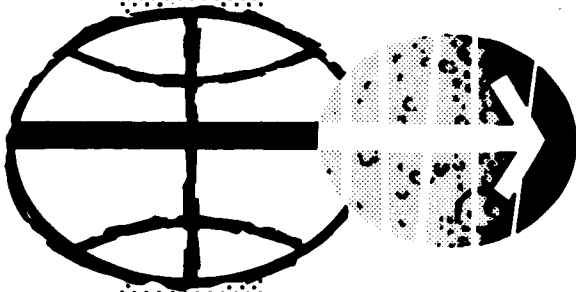
APOLLO 14 MISSION REPORT  
SUPPLEMENT 8

SUMMARY OF APOLLO EXPERIMENTS  
ON  
LAUNCH PHASE ELECTRICAL PHENOMENA

**CASE FILE  
COPY**

DISTRIBUTION AND REFERENCING

This paper is not suitable for general distribution or referencing. It may be referenced only in other working correspondence and documents by participating organizations.



MANNED SPACECRAFT CENTER  
HOUSTON, TEXAS  
JULY 1972

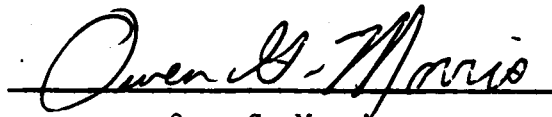
APOLLO 14 MISSION REPORT  
SUPPLEMENT 8

SUMMARY OF APOLLO EXPERIMENTS ON LAUNCH PHASE ELECTRICAL PHENOMENA

PREPARED BY

Apollo Mission Evaluation Team

APPROVED BY

  
Owen G. Morris  
Manager, Apollo Spacecraft Program

NATIONAL AERONAUTICS AND SPACE ADMINISTRATION  
MANNED SPACECRAFT CENTER  
HOUSTON, TEXAS  
JULY 1972

## SUMMARY OF APOLLO EXPERIMENTS ON LAUNCH PHASE ELECTRICAL PHENOMENA

### INTRODUCTION

As a result of the electrical disturbances experienced during the Apollo 12 launch, the value of further research in this area was recognized and several experiments were performed prior to, during, and subsequent to the Apollo 13 and Apollo 14 launches to study certain aspects of launch phase electrical phenomena. The Apollo 13 experiments were performed primarily to study the effects of the space vehicle on the atmospheric electrical field during launch. To better define the origin of the electrical charge and the triggering mechanism of the discharge, additional experiments were performed in connection with the Apollo 14 launch.

The experiments were conducted by several organizations under contract to the National Aeronautics and Space Administration. Atmospheric electrical field measurements were made by the New Mexico Institute of Mining and Technology and by the Stanford Research Institute; low-frequency and very-low-frequency radio noise measurements were made by the Stanford Research Institute to detect corona discharges indicative of high vehicle potential; and radiometric measurements of the launch vehicle exhaust temperature were made by the Lockheed Electronics Company to calculate the Apollo vehicle exhaust breakdown electric field strength. In addition to these experiments, measurements were made by the Westinghouse Research Laboratories subsequent to Apollo 14 to acquire data for the derivation of peak current in lightning strokes. This report, which constitutes supplement no. 8 to the Apollo 14 mission report, summarizes these experiments and the conclusions reached.

ATMOSPHERIC ELECTRICAL FIELD EXPERIMENT<sup>a</sup>

## Purpose

The atmospheric electrical field experiment was conducted during the Apollo 13 launch to measure the electrical perturbations produced by the Apollo vehicle. The measurements showed the presence of a much stronger electrical disturbance than had been expected, and that the disturbance may have been caused by a buildup of electrostatic charges in the launch vehicle engine exhaust clouds, charge buildup on the vehicle itself, or a combination of both. The experiment was continued during the Apollo 14 launch to define the origin and carriers of the charge.

## Experiment Configuration

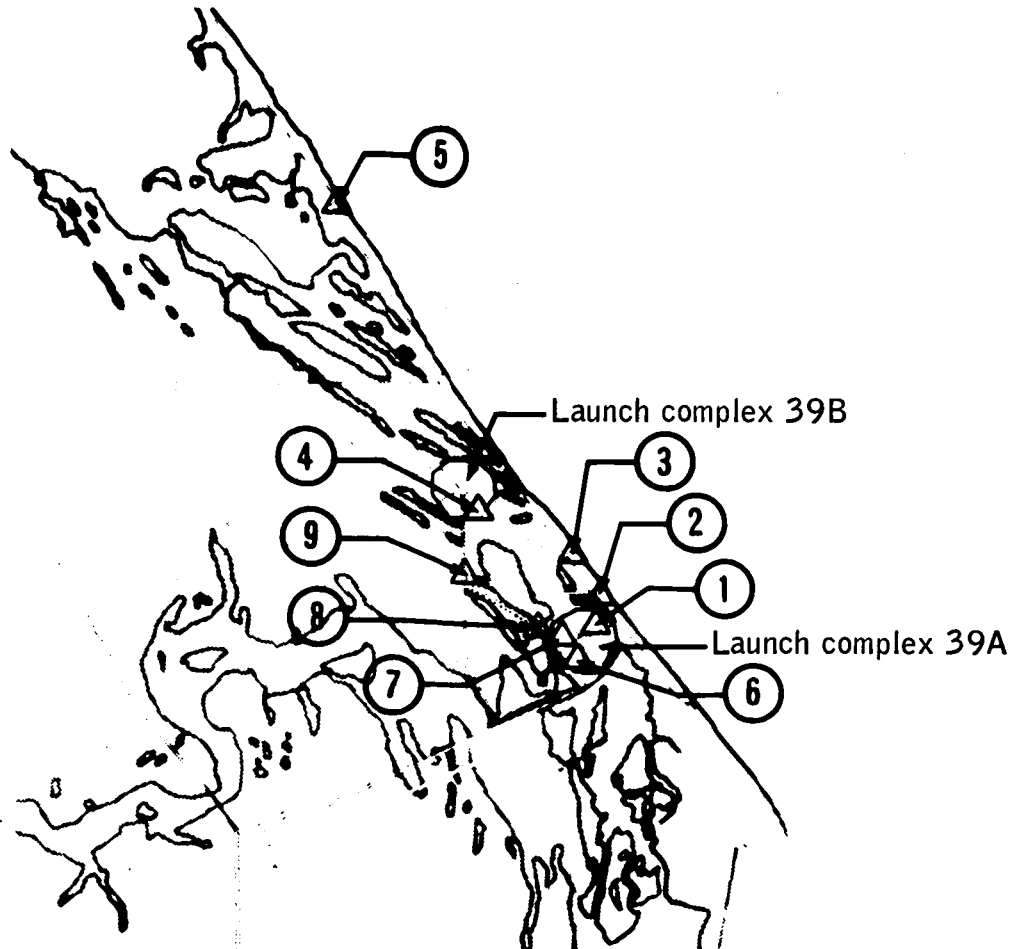
Figures 1 and 2 show the network of nine calibrated electrical field meters installed for the Apollo 13 launch. Fourteen field meters (fig. 3) were installed for the Apollo 14 launch, including one on the launch umbilical tower (fig. 4) to detect any charge buildup on the vehicle during ignition and during the initial seconds after lift-off. Accurate timing signals, which were not available for Apollo 13, were provided at most of the Apollo 14 field measurement equipment locations. Time-lapse photographs of the launch vehicle exhaust clouds were also taken during the Apollo 14 launch to aid in the interpretation of the data.

## Observations and Data

Apollo 13.— Data from the electrical field instruments during the Apollo 13 launch are shown in figure 5. Very large perturbations of the normal electric field were recorded on meters at sites 1, 2, and 3. The data from these sites show a rapid increase in the positive direction, followed by a slower decrease. Data from site 4, however, do not indicate significant variation in field intensity.

Excellent records at several sensitivity levels were obtained at site 7. The field perturbation immediately following launch rose to a maximum of 1200 volts/meter in the positive direction about 25 seconds

<sup>a</sup>Data included in this section were extracted from reports submitted by M. Brook, C. R. Holmes and C. B. Moore of the New Mexico Institute of Mining and Technology, and by J. E. Nanevich, E. T. Pierce, and A. L. Whitson of the Stanford Research Institute.



Field meter no.	Distance from launch complex A, meters	Azimuth, deg
New Mexico Tech		
1	415	46
2	730	33
3	1500	355
4	2200	325
5	7780	338
Stanford Research Institute		
6	400	183
7	380	265
8	850	289
9	1810	290

Figure 1.- Field meter network for Apollo 13 launch.

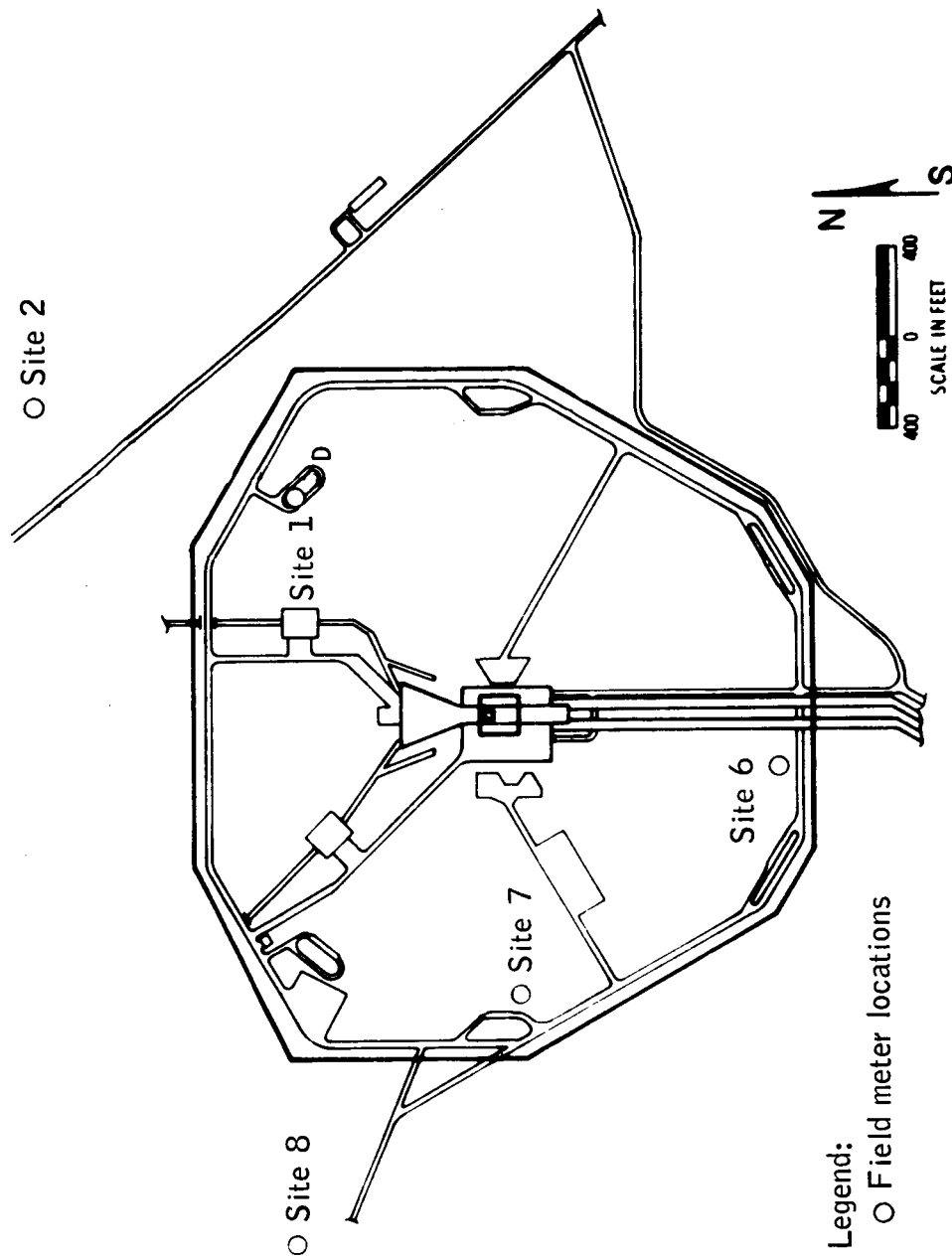


Figure 2.- Field meter locations in the proximity of the launch complex for Apollo 13.

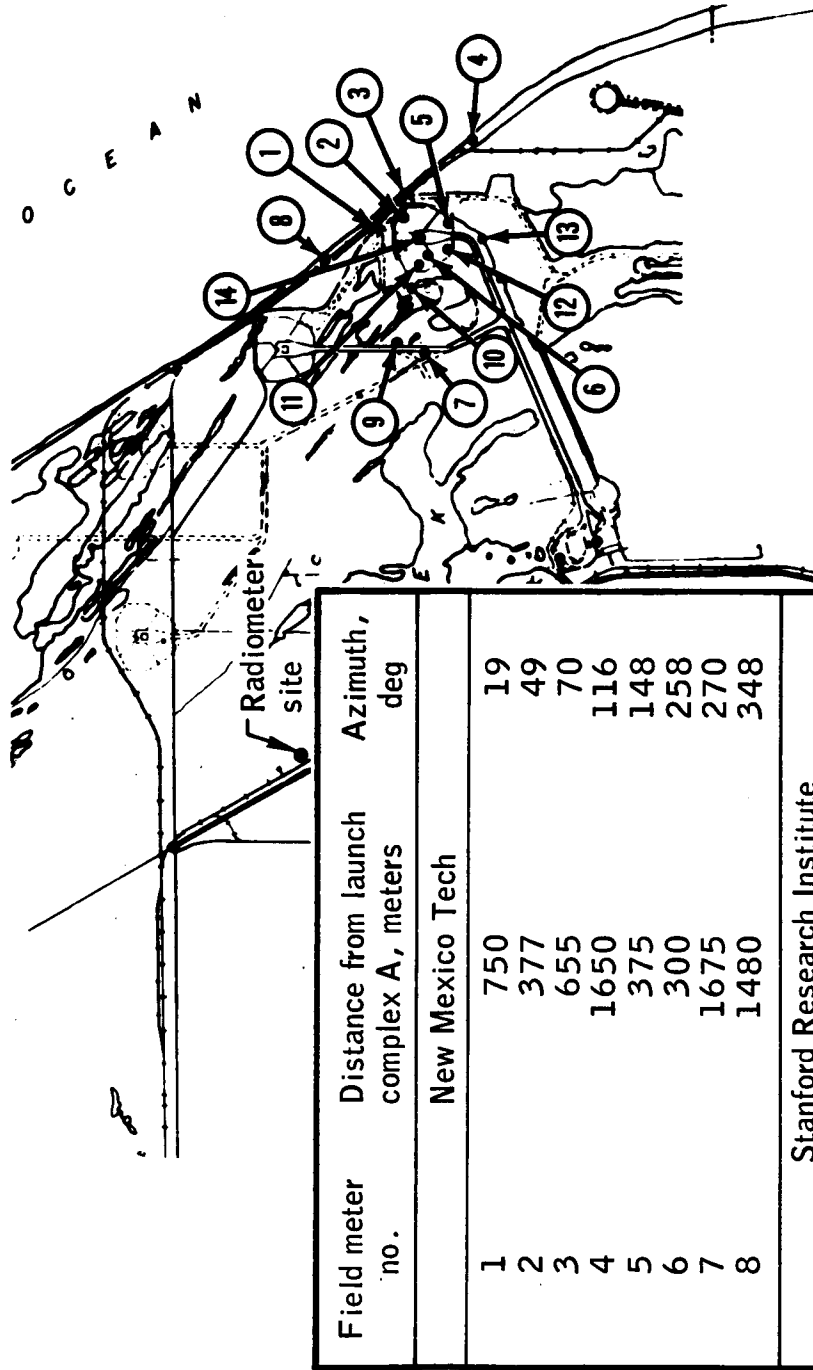


Figure 3.- Field meter network and radiometer site for Apollo 14 launch.

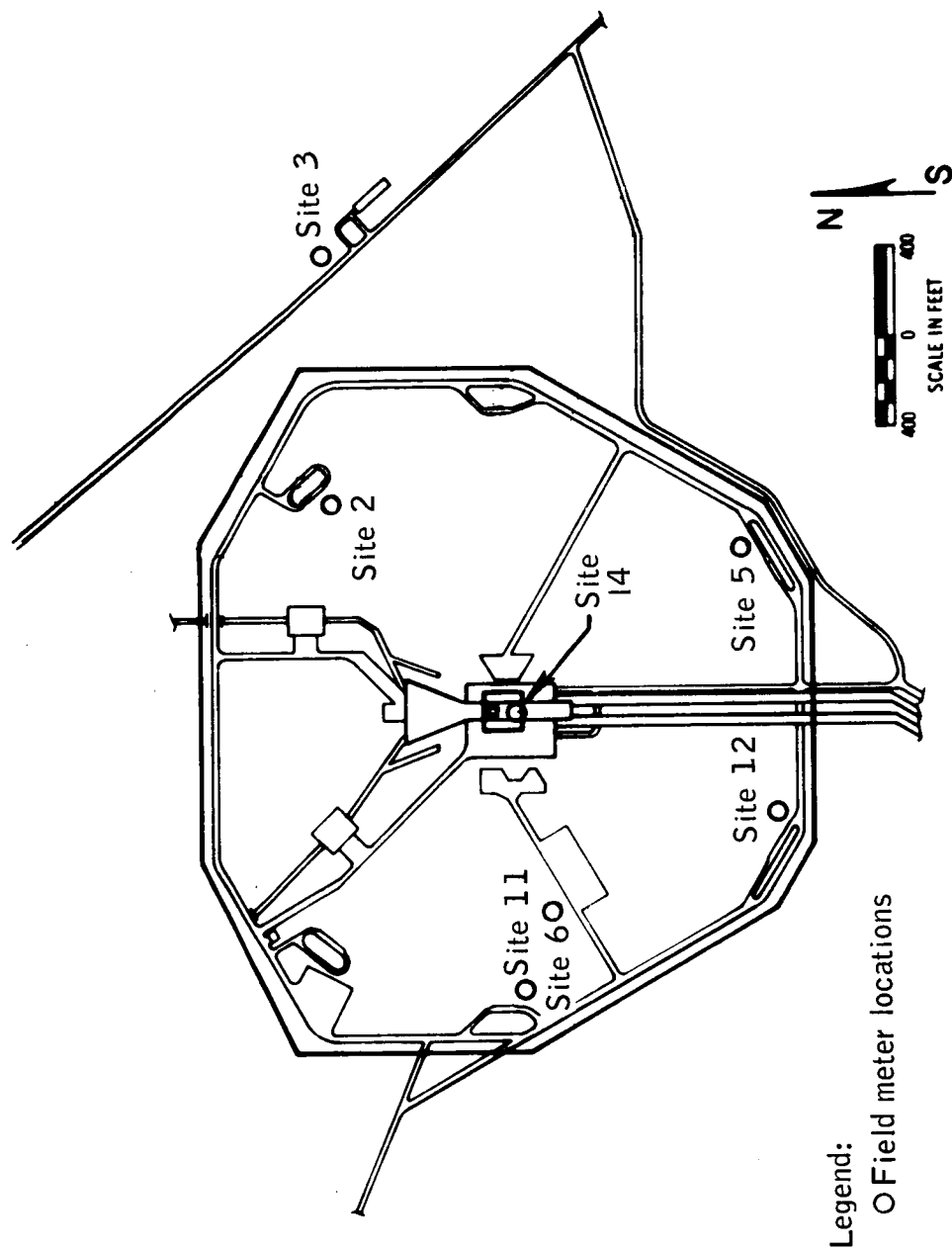
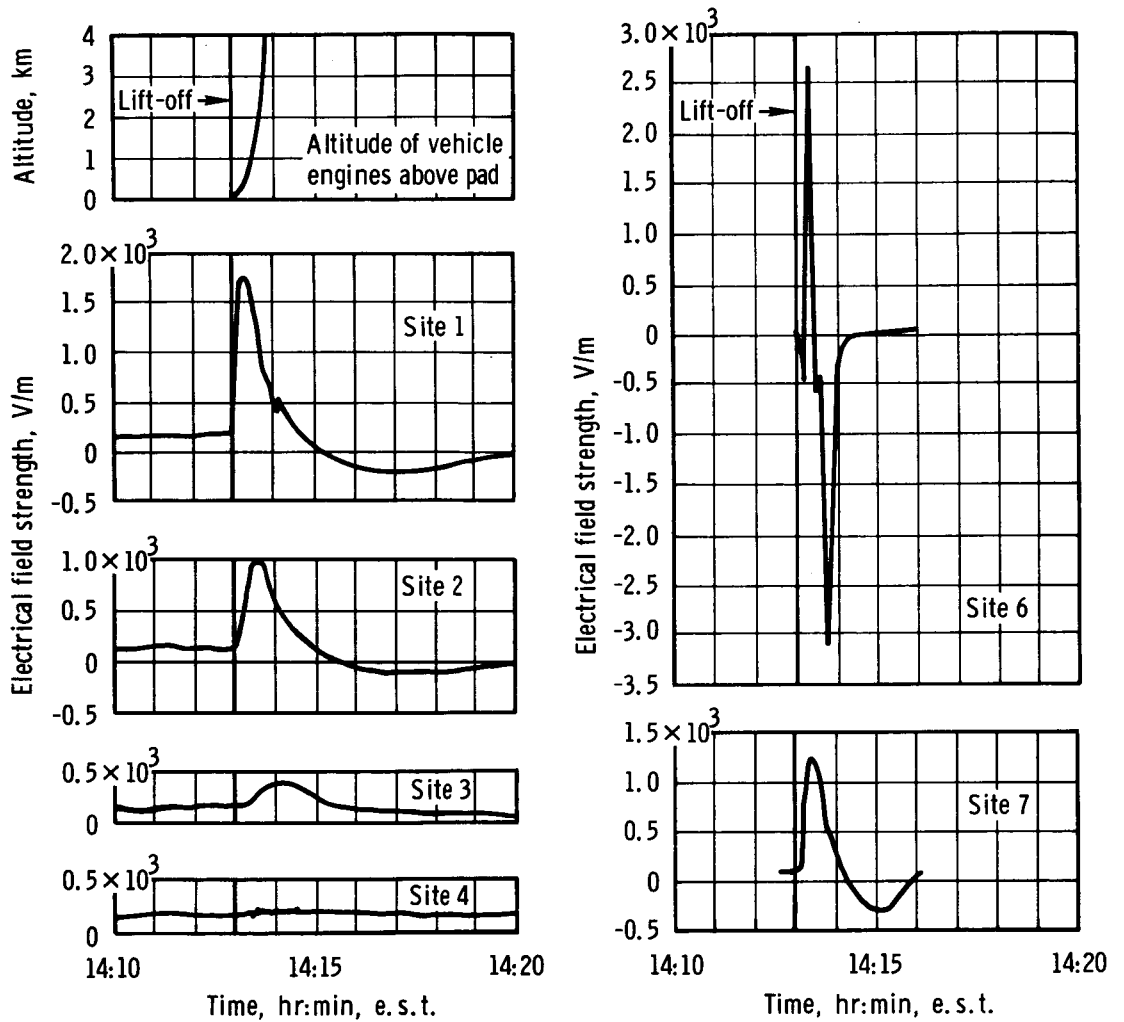


Figure 4.- Field meter locations in the proximity of the launch complex for Apollo 14.





Note: Locations of sites are shown in figure 1.

Figure 5. - Electrical field data during Apollo 13 launch.

after lift-off, then reversed, reaching a negative peak of some 300 volts/meter about 115 seconds after lift-off. Thereafter, the field gradually returned to the unperturbed value. The record at site 6 was similar to that at site 7, with an initial positive excursion followed by a slower negative excursion. This record, however, shows larger fluctuations, which could have been caused by gravel and dust stirred up by the exhaust of the launch vehicle engine. (After launch, a quantity of such debris was found in the vicinity of the field meter.) A large negative field of approximately minus 3000 volts/meter was recorded 40 seconds after lift-off which probably resulted from the exhaust and steam clouds that tended to remain over site 6.

Access restrictions to sites 8 and 9, required that the recorders for these sites be started several hours prior to launch. Unfortunately the strip charts had stopped feeding before lift-off. However, both positive and negative field measurements were recorded on the stalled charts. The magnitude of the electrical field was greater than any that had been previously recorded at any point on the strip chart. Examination of these records from sites 6 and 7 indicated that the only large field perturbations were those accompanying launch. Therefore, the peak excursions of the records at sites 8 and 9 can be assumed to have occurred just after lift-off.

Apollo 14.- Prior to the Apollo 13 launch, (14:13:00 e.s.t. on April 11, 1970), the field meters had shown fluctuations of 100 to 200 volts/meter. Twenty minutes prior to the scheduled Apollo 14 launch, cumulus clouds existed in the launch complex area with tops at 4600 meters. Ten minutes later, the cloud tops were at 5500 meters. The electric field meters clearly showed fluctuating fields, characteristic of mildly disturbed weather condition during this time. Since the mission rules did not allow a launch through cumulus clouds with tops in excess of 3050 meters (10 000 ft) a 40-minute hold was required before a permissible weather situation existed. At the time of lift-off of Apollo 14 (16:03:02.6 e.s.t. on January 31, 1971), the sky was overcast with a few breaks in the clouds, and the altitude of the cloud bases was about 1500 meters above sea level. The surface winds were brisk at about 6 meters/second from an azimuth of about 260°. The wind speed at the top of the launch umbilical tower (a height of about 130 meters) was blowing at about 12 meters/second from an azimuth of about 270°. During this period, a weakly electrified cloud cell to the north of the launch complex was being blown toward the coast.

The exhaust from the Apollo 14 space vehicle produced large clouds. Initially, the major cloud was the one that issued with the exhaust flame from the southern end of the flame trough. The section of the trough slopes upward toward the south so that it deflects the exhaust at an angle of about 20° above the horizontal. The deflected flame extended south

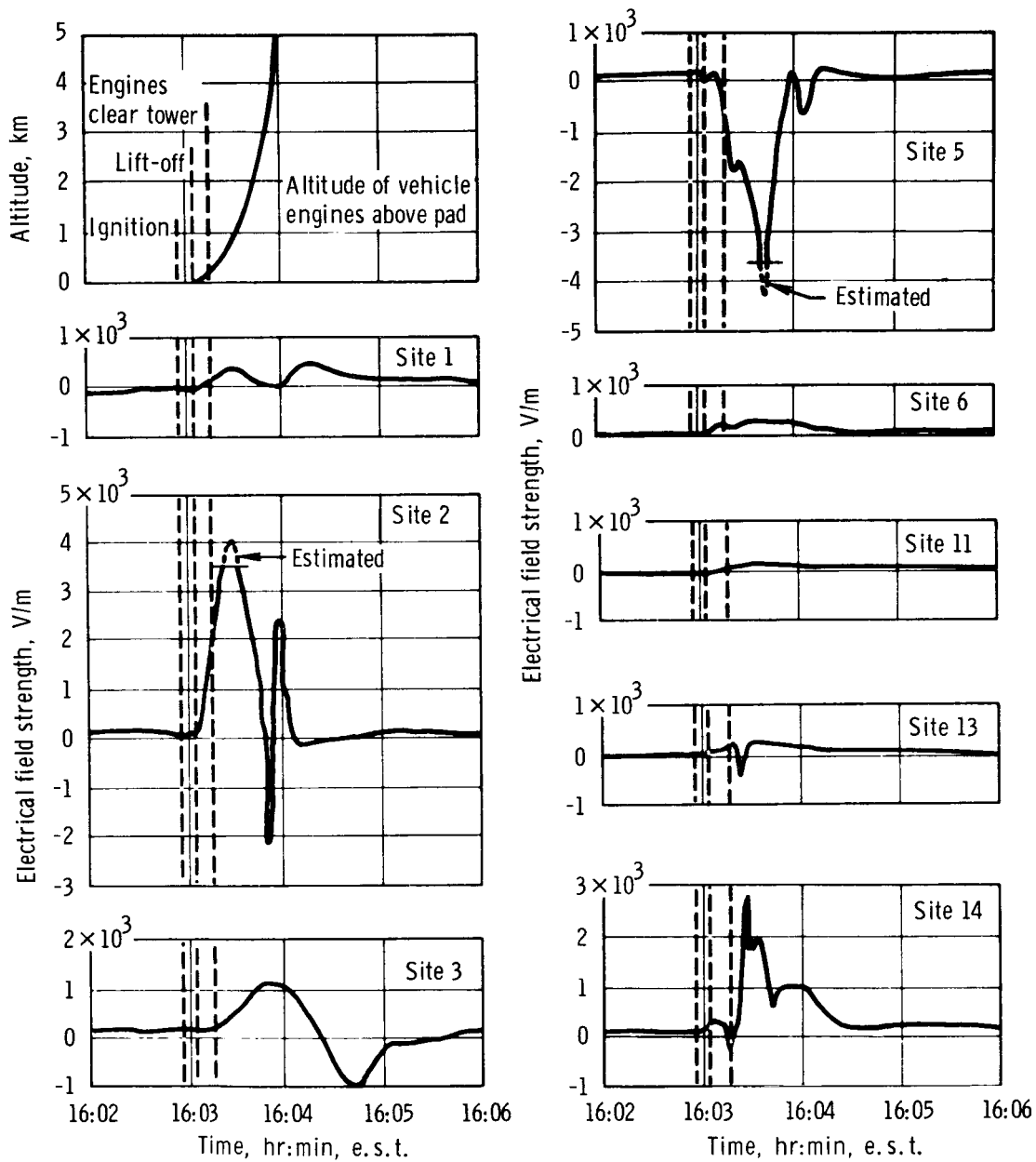
from the vehicle for about 400 meters; however, a yellowish cloud was projected much further south. The cloud rose rapidly with an initial speed of about 16 meters/second while moving eastward with the wind. An electric field meter under the path of the exhaust cloud and inside the launch perimeter fence (site 5 shown in fig. 4) recorded the presence of a strong negative charge in the cloud with a field strength of about 4500 volts/meter (fig. 6). The recording of a negative charge continued for about 47 seconds. Wind measuring equipment near site 5 indicated the presence of a strong gust of wind from the northeast with a speed of 11 meters/second about 10 seconds after the aforementioned negative charge indication. A new local field excursion caused by negative charge above site 5 appeared at the time of the wind gust (fig. 6). The negative charge in the cloud disappeared rapidly as evidenced by a very small perturbation that was recorded when the cloud passed the southernmost field meter at site 4 on the coast (fig. 3) 30 seconds later.

Motion pictures taken with a camera pointed downward from the top of the launch tower toward the south indicate that very little cooling water was injected onto the pad south of the tower; the pad surface appears red hot. Debris deposited on the instruments at site 5 appeared to be fragments of fire brick and other non-aqueous solid materials.

The northern opening of the flame trough directs the main exhaust cloud horizontally. Spray nozzles are arranged here to inject several tons of water per second into the cloud. Initially, the large cloud of exhaust and steam which formed during ignition and lift-off rose slowly with its center about 400 meters north of the launch umbilical tower. This cloud grew to be quite large and rose at about 10 meters/second as it was carried by the wind toward the coast. The cloud contained a dominant positive charge that produced a peak electrical field intensity at site 2 (figs. 3 and 6) of about 4100 volts/meter. The effects of this charge were much more persistent than were those of the negative charge in the southern cloud as perturbations caused by positive charge were detectable at sites 4 and 8 after the negative charge had been neutralized.

The field records from sites 1 and 2 show transient perturbations superimposed on the excursion produced by the dominant positive charge in the northern cloud. These were apparently produced by local concentrations of negative charge. The data are not sufficient to identify the cause of these perturbations. They indicate, however, a complex distribution of charge in the exhaust cloud and several different sources of charge.

The field records from sites 2 and 3 (fig. 6) show the effect of the dominant positive charge in the northern cloud followed by the effect of negative charge over the sites. (Time-lapse photographs show a low-level cloud or spray that extended out to site 3 at about the time of the negative excursion.)



Note: Locations of sites are shown in figure 3.

Figure 6. - Electric field data during Apollo 14 launch.

### Analysis

The following observations guided the analysis of the Apollo 14 data:

1. On the evening following the Apollo 14 launch, an examination of the field meter ground plane and sand bag buttress at site 5 revealed a greyish white deposit composed of particles ranging in size from dust particles to some having diameters exceeding  $3/8$  inch.
2. As mentioned previously, the film record obtained with the camera pointed down and toward the south side of the launch umbilical tower revealed that the flame trough on the south side was red hot. It also showed that the cooling water was not turned on at ignition, but was turned on as the vehicle ascended. Time-lapse photographs also show that the launch umbilical tower cooling water was not released in very great quantity until some 20 seconds after ignition.
3. Time-lapse photographs show that a low-level cloud originated at the launch umbilical tower after lift-off and extended out to at least site 3 at the same time the north cloud base was well above the height of the launch umbilical tower.

In an attempt to analytically duplicate the recorded data, a model defining the boundaries and motions of the northern and southern clouds was developed and the net field at each of seven stations was calculated. The next step was to assume that the north and south clouds moved as observed, but with constant charge. Under these conditions, it was not possible to reproduce the details of the field records seen at sites 2 and 5; however, a similarity to the fields measured at sites 4, 6, and 8 was evident. Also noticeable was the fact that the southern cloud affected site 5, primarily, and had little influence on other field meter sites.

The calculations were refined by assuming that charged particles began to fall out of the southern cloud 15 seconds after lift-off with a fall rate of 6 meters/second. With this assumption, the field recorded at site 5 was approximated. It is interesting to note that the abrupt change in wind direction at the time of the final negative excursion recorded at site 5 (fig. 6) would have resulted in additional fallout to the area around site 5 and provides a much closer approximation of the recorded data. The red-hot flame trough shown in photographs gives credence to the supposition that particles of fire brick and other debris were carried up into the southern cloud and subsequently fell out. The model indicates that the effect of the southern cloud on site 6 was negligible because the cloud was blown to the east before it got very high. Also, the launch umbilical tower may have had a shielding effect.

The presence of a third cloud carrying negative charge is necessary to explain the negative excursions at sites 1, 2, and 3. The time-lapse photographs clearly show that the launch umbilical tower cooling water was the origin of a third cloud. The required negative charge can be attributed to the strong positive field of the northern cloud inducing a negative charge in the water spray droplets. Using a line-charge model for the launch umbilical tower water cloud, added to the effects of the northern and southern clouds, it is possible to calculate the observed negative excursions at sites 2 and 3. The negative excursion at site 1 cannot be accounted for other than by concluding that a local perturbation was present.

The field meter on the Apollo 14 launch umbilical tower indicated a small positive value ( $<400$  volts/meter) a few seconds after lift-off. Model measurements using a 1/144-scale model of the launch umbilical tower and the Apollo/Saturn vehicle indicate that, in this configuration, the launch umbilical tower field and the vehicle potential are related by volts/field = 20 meters. Thus, the vehicle potential is calculated to be less than 8000 volts (400 volts/meter multiplied by 20 meters).

During the Apollo 13 launch, the instruments at sites west of the launch complex registered a smooth positive field increase, succeeded by a less pronounced negative excursion. For Apollo 14, the negative excursion was not evident; however, the field variations occurred at approximately equivalent times for both launches. The positive excursion was approximately five times greater for Apollo 13 than for Apollo 14, and reached maximum when the space vehicle was at altitudes greater than 1000 meters. This observation, coupled with the fact that the maximum electrical fields were observed downwind on both launches, makes it unlikely that the space vehicle charge was the dominant factor but, rather, that the charged clouds were the dominant sources of the electric fields.

### Results

Apollo 13.— The Apollo 13 field meter records show that the launch of the space vehicle produced a significant separation of electrical charge. However, because of the absence of accurate timing signals and time-lapse photography of the vehicle exhaust clouds, the distribution of charge could not be ascertained. Nevertheless, the data were useful in showing that the separation of electrical charge produced at launch could contribute to the hazard of launching in a marginal weather situation, and they were also useful in the interpretation of the Apollo 14 data.

Apollo 14.-- The analysis of the Apollo 14 records indicated three major sources of electrification, all in the form of charge transported by clouds. The following values of charge were calculated from the available data.\*

- a. Northern cloud - 45 millicoulombs positive
- b. Southern cloud - 3 millicoulombs negative
- c. Launch umbilical cooling water cloud - 3 millicoulombs negative.

The charge on the Apollo 14 vehicle appears to make a negligible contribution to the measured fields. A comparison of the launch umbilical tower record with the data from the other sites indicated that the charge on the Apollo 14 vehicle, during the initial stages of ascent past the launch umbilical tower, was only on the order of 10 microcoulomb; this is compatible with the belief that the exhaust is a good electrical conductor over a distance of about 100 meters.

#### RADIO-FREQUENCY NOISE EXPERIMENT<sup>a</sup>

##### Purpose

Instrumentation for both the Apollo 13 and Apollo 14 atmospheric electricity measurements included provisions for the measurement of RF noise in the frequency range from 1.5 to 120 kHz. The rationale for these measurements was that, since the vehicle was not instrumented for onboard measurement of vehicle potential, various provisions for remotely sensing the effects of high vehicle potential should be included in the ground instrumentation. It was theorized that, if the vehicle reached sufficiently high potentials after launch, corona discharges from the vehicle structure would occur. If noise generated by these discharges could be detected, it would be an indication that the vehicle potential had reached the corona threshold of some part of the vehicle structure.

##### Experiment Configuration

Apollo 13.-- The noise measuring instrumentation for Apollo 13 consisted of a loop antenna (located near site 7 in fig. 2) feeding a set of five fixed-tuned receivers. The output of each receiver was recorded on one channel of a strip chart recorder also used to record site 7 static

\*Calculations were made by M. Brooks.

<sup>a</sup>Data included in this section were extracted from a report submitted by J. E. Nanevich, E. T. Pierce and A. L. Whitson of the Stanford Research Institute.

electric field data. Unfortunately, the experiment was planned so near the launch date that it was not possible to provide range timing signals to the recorders.

Apollo 14.- To gain additional confidence in the functioning of the noise measuring system, provisions were made on the launch of Apollo 14 to use a broadband tape recorder to record the output of the loop antenna preamplifier. This technique eliminates microphonics generated within the receivers by the high acoustic noise fields associated with the launch. In addition, an electric-dipole-type antenna system was installed near the loop antenna location. This provided a completely independent source of RF noise data from receiving antenna through recorder. To provide information on vibrational noise levels, an accelerometer was installed on the loop antenna preamplifier housing and its output was recorded on a trace of the tape recorder. Finally, timing signals were provided to both the tape recorder and the strip chart recorder.

#### Data

Apollo 13.- Noise data obtained during the Apollo 13 launch are shown in figure 7. Since range timing data were not recorded, it was necessary to extrapolate the recorded data to establish an absolute time base. The noise record showed that a marked offset in the levels of the four highest frequency noise channels occurred shortly before the pronounced change in the electric field. This change in noise level was thought to have been caused by the charged vehicle clearing the launch pad. Accordingly, lift-off time on the record was set at the time of the noise level change.

Apollo 14.- The RF noise measurement strip chart recorder output data, obtained during the Apollo 14 launch, are shown in figure 8. These records, obtained using the loop antenna, indicate a large increase in noise on the 1.5-kHz and 6-kHz channels 3 seconds after ignition, while the 51-kHz channel noise did not begin until 2 seconds after lift-off. This behavior is quite different than that illustrated in figure 7 where the initial change in noise level occurred simultaneously on all channels from 6 kHz through 120 kHz, and the peak of the perturbation in 1.5-kHz noise level occurred 25 seconds later. To validate the Apollo 14 strip chart noise data, the noise receivers used during the launch were set up in the laboratory; the tape-recorded broadband noise data obtained from loop antenna preamplifier and from the electric dipole antenna preamplifier during the launch were then fed into the receivers. The receiver outputs obtained during this experiment are shown in figure 9.

It is of interest, first, to compare the loop antenna data of figure 9 with that of figure 8. The two records display the same general signal level variations demonstrating that receiver microphonics did not appreciably influence the data of figure 8. Next, a comparison was made of the



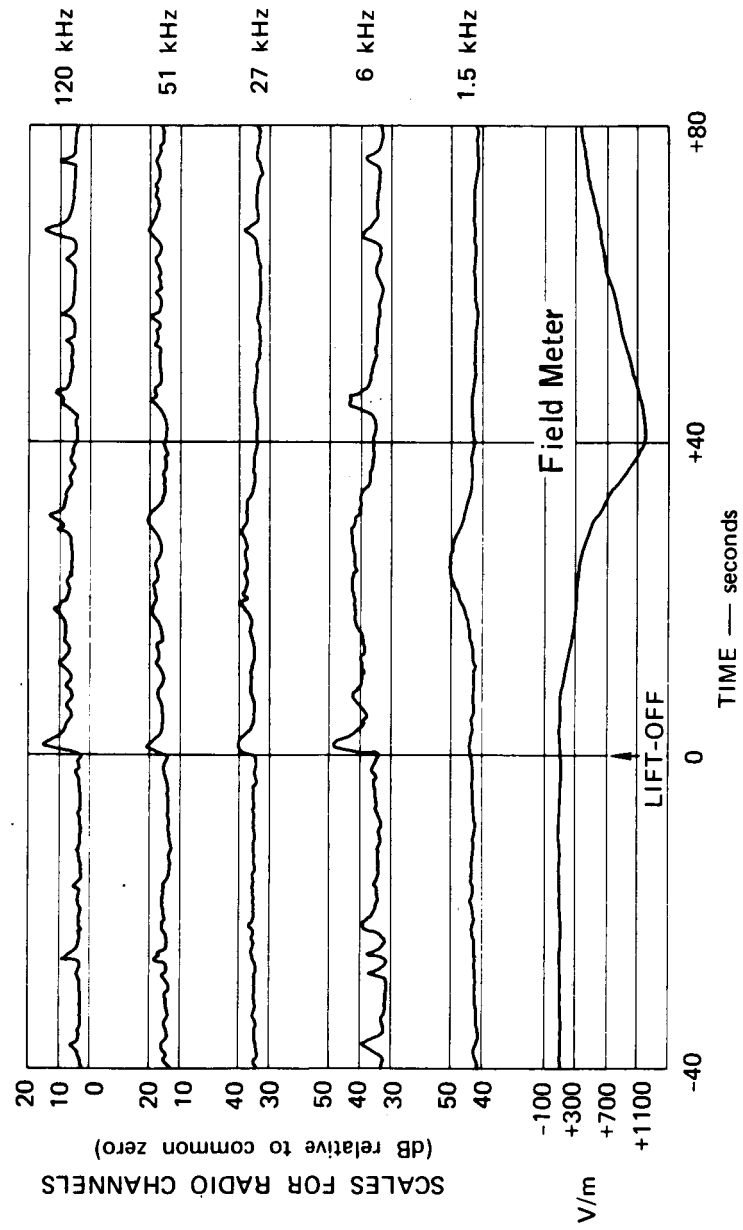


Figure 7.- Noise and field meter records from site 7 during launch of Apollo 13.

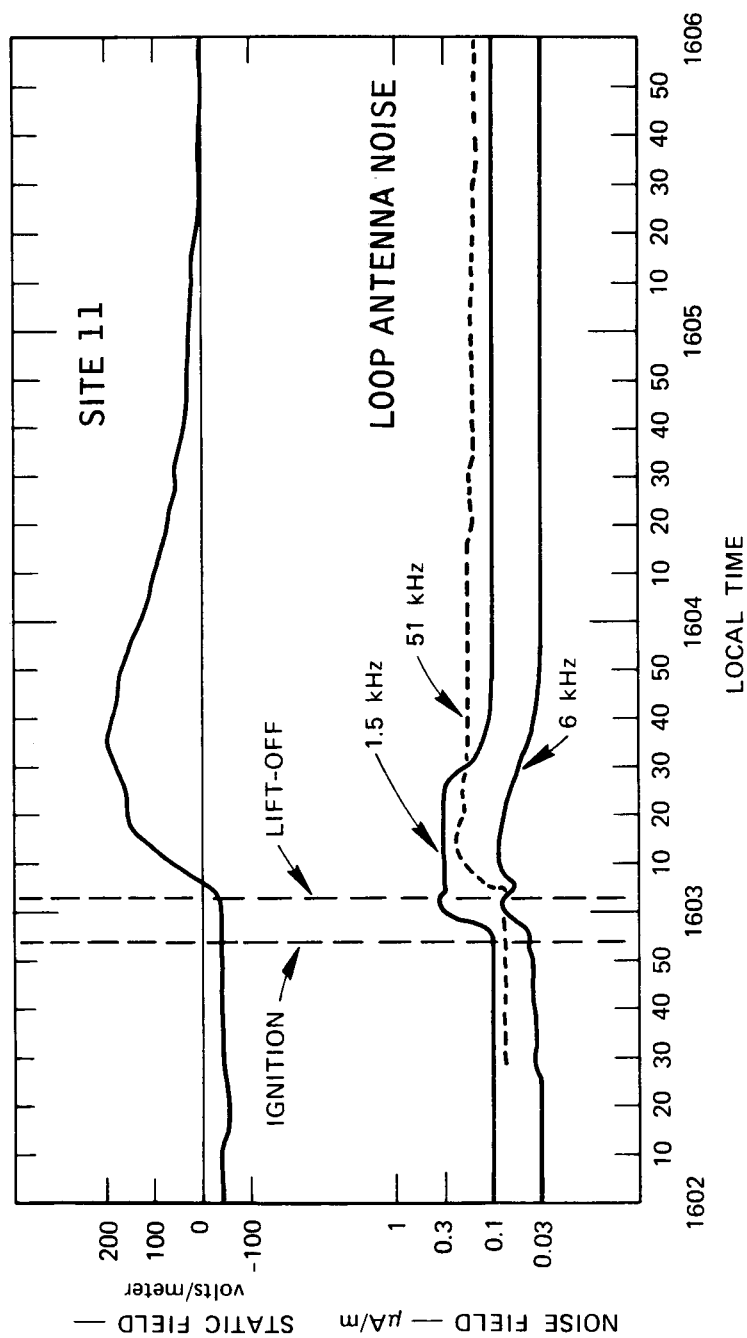


Figure 8.- Strip chart recorder noise and field meter records from Apollo 14 launch.

loop and electric dipole antenna data in figure 9. Again, the field intensity records are in good agreement. Since completely different sensors and antenna preamplifiers were used in obtaining these data, this agreement means that preamplifier or antenna microphonics can also be discounted as having influenced noise field intensity data. Thus, the RF noise records of figures 7 through 9 can be considered to be representative of the true radio noise environment during launch.

Since the 1.5-kHz and 6-kHz noise started shortly after Apollo 14 ignition, this noise might be attributed to plasma processes occurring in the exhaust. Because 51-kHz noise did not occur until after lift-off, it was felt that it might be ascribed to voltage breakdown processes associated with vehicle charging after launch. Unfortunately, the 51-kHz noise started at 16:03:05 e.s.t., before the space vehicle had cleared the launch umbilical tower; and, according to field meter launch umbilical tower data, the vehicle potential at that time was apparently too low to support substantial noise-producing breakdowns from the vehicle.

In an effort to extract additional information from the RF noise records, a rayspan readout was made of the wideband tape recordings of both the loop and electric dipole noise. The rayspan data are shown in figure 10, in which time is plotted along the horizontal axis, frequency is plotted along the vertical axis, and noise field intensity is proportional to the darkness of the trace. In order to assess the characteristics of the vibrational environment at the loop antenna base, a rayspan readout was also made of the accelerometer signal and is shown in the lower portion of figure 10. The figure indicates that there was a marked change in the launch pad electromagnetic environment near the time of launch. (The record also indicates that data were not generated by microphonics because there is no correlation between the RF noise data and the accelerometer signal.) At 16:02:33 (21 seconds before ignition) broadband white-noise-like interference becomes evident on the electric dipole data in figure 10. A little later, at 16:02:38 (16 seconds before ignition) four discrete signals appear, starting at zero frequency and, in 1 second, sweeping up in frequency to rest at 2.5, 5.0, 7.5 and 10.0 kHz, as though some high-inertia device such as a motor were being brought up to speed. These signals appear to stop abruptly at 16:04:03. Additional discrete signals appear at 16:02:49 (5 seconds before ignition). Another group of roughly five upward-sweeping discrete signals appear at 16:02:51 (3 seconds before ignition). These signals are indicative of starting of high inertia devices associated with various activities such as turning on pumps, recorders, etc. immediately prior to launch

Three and one-half seconds after ignition (at 16:02:57.5), some broad signals centered about discrete frequencies, appear at low frequencies in figure 10 (particularly on the loop antenna). It is apparently these latter broad signals which were responsible for the signal strength records

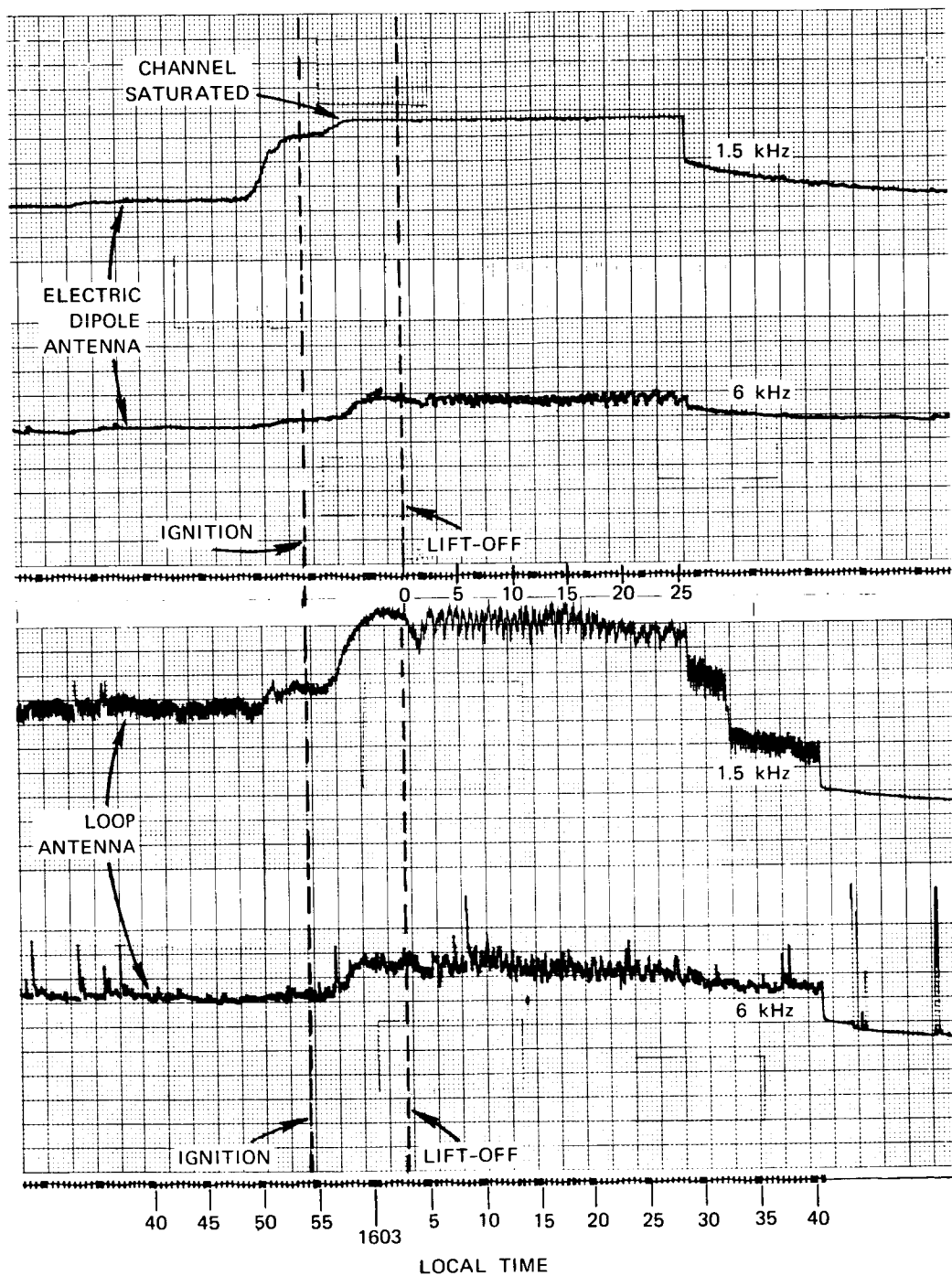


Figure 9.- Apollo 14 radio noise signal strengths from broadband tape recorder data.

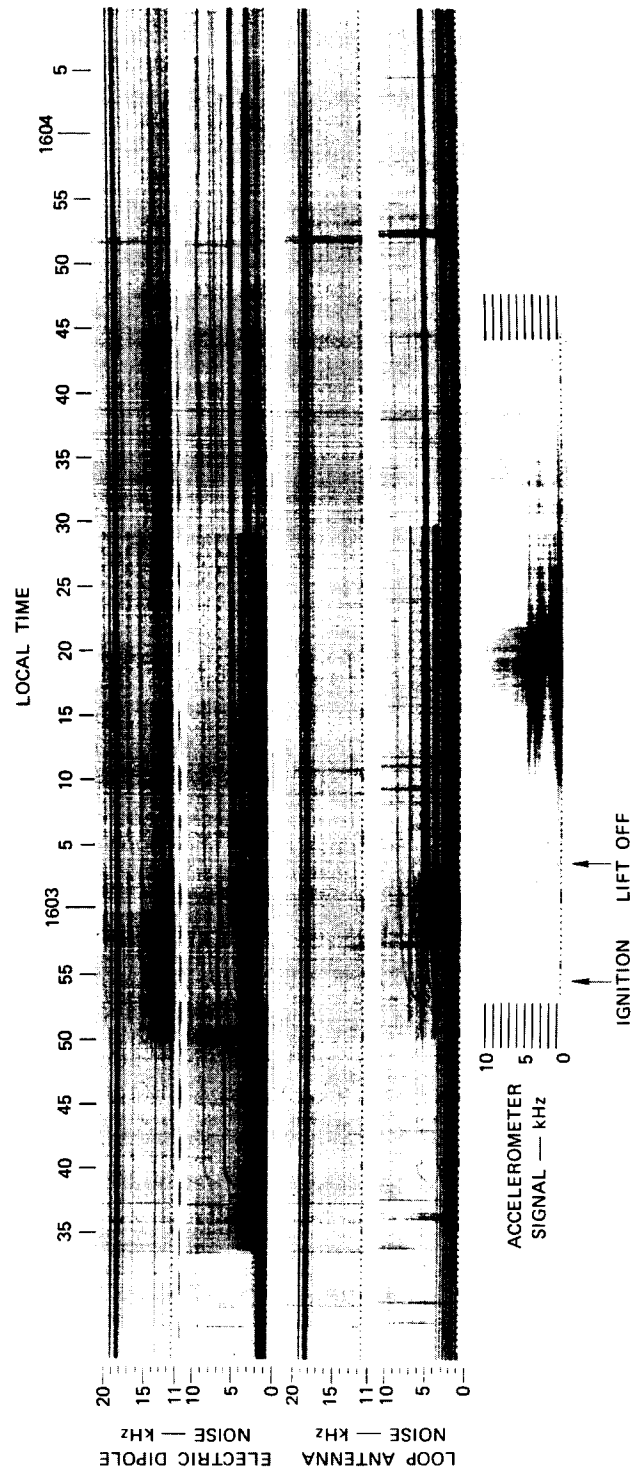


Figure 10.- Signals measured during launch of Apollo 14.

obtained on the 1.5- and 6-kHz noise receivers (fig. 9) because large increases in signal strength occurred on the receiver records at 16:02:57.5. Some of these broad, but discrete, noise signals are clearly modulated at a rate varying from 1 Hz to 2 Hz starting at 16:03:05.4. This modulation is evident in figure 9 as a series of peaks in the 1.5-kHz loop antenna signal level starting 16:03:05.5. This same modulation is evident in the 6-kHz electric dipole record, but not in the 1.5-kHz dipole channel, which was saturated at this time. The modulated noise signals disappear abruptly at 16:03:28.8 in the rayspan record of figure 10. This corresponds to the first abrupt drop in the 1.5-kHz loop antenna signal level which occurs at the same time. It should be noted that the rayspan readout has a limited dynamic range so that if the gain of the system had been increased, the records would be generally darker, but the records might indicate that some signal persisted at 1.5 kHz after 16:03:28.8, in agreement with the field strength record of figure 9.

### Analysis and Results

Analysis of the records with respect to the launch events revealed the following.

The Apollo 13 radio noise measurements indicated that a change in the low-frequency RF noise level occurred at the general time of launch, and that the noise persisted for a period of roughly 35 seconds after onset. Rudimentary shock tests were conducted to establish whether the trace deflections resulted from RF noise or from microphonics (or some other process in the receiving system) so that the noise data might provide insight into the static charging of the vehicle. The tests revealed no microphonics noise capable of producing the observed traces. Accordingly, it was decided that the recording trace offsets were caused by RF noise associated with the launch.

The noise started after ignition and changed character 2.4 seconds after lift-off when the vehicle was 4.25 meters off the pad. It persisted until almost 30 seconds after launch at which time the vehicle entered the bottom of the cloud deck at an altitude of 4000 feet. Since, from figure 9, the signal level of this noise was virtually unchanged until the vehicle was at 4000 feet altitude, it is difficult to see how a source on the vehicle itself could be solely responsible for the observed signal. If the source were on the vehicle, one would expect a considerable reduction in signal strength as the vehicle climbed.

Another possible source of this noise is the launch pad water systems which operated over roughly the same time interval as the noise. Figure 11 shows that, on Apollo 13, the flame trench system B and launch umbilical

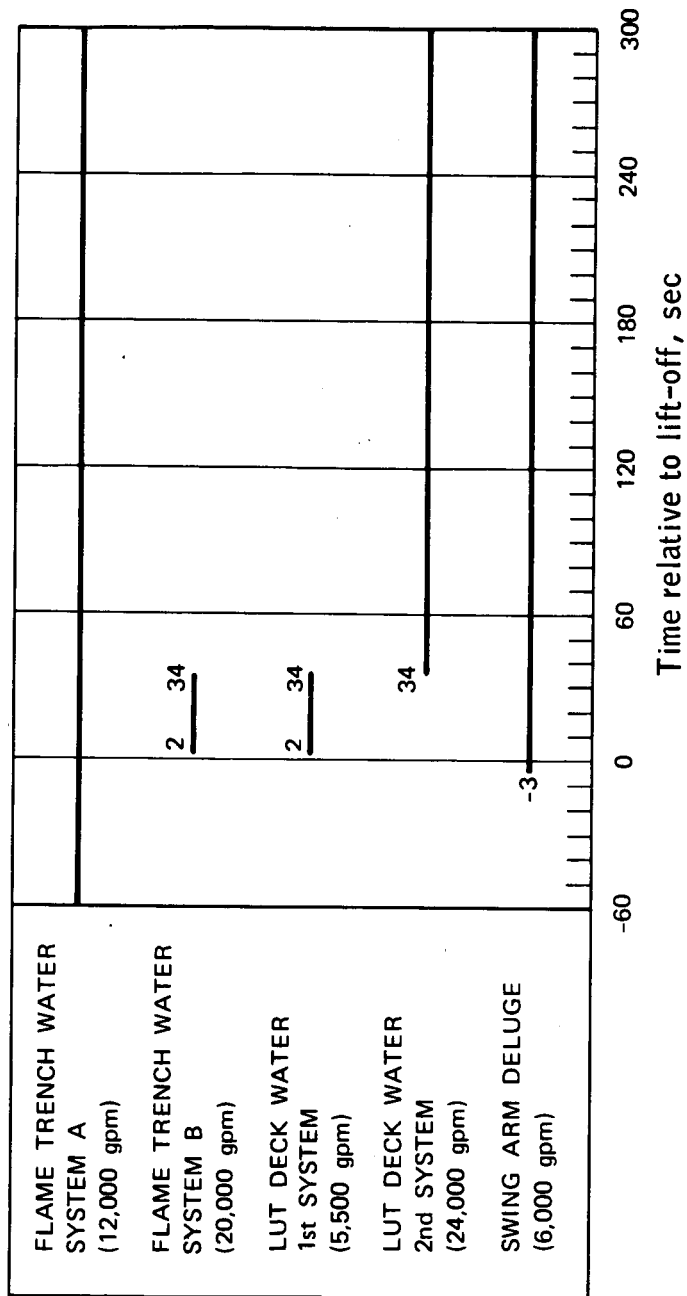


Figure 11.- Activity of pad water deluge system on Apollo 13 launch.

tower deck first system were both on from 2 seconds prior to lift-off until 34 seconds after lift-off. It is known that sprayed water becomes charged, and the resultant field intensities can become sufficiently high for RF-noise-producing electrical breakdowns to occur (ref. 1). Also, the electrostatic field measurements show conclusively that the clouds, produced by the interaction of the hot exhaust with the water and the flame trenches, were highly charged. It is plausible that breakdowns generating radio noise could have occurred within these clouds. The exact manner, however, in which these processes would operate in the high-temperature lift-off environment is not understood. Electrification and noise existed with water systems that functioned from 2 to 34 seconds after lift-off. This was not evident with the water systems that were operating at various times from minus 60 to plus 300 seconds from lift-off. This phenomenon is not currently understood.

In conclusion, on the basis of the meager Apollo 13 RF noise data and the more substantial Apollo 14 data, in the frequency range studied, the RFI generated near launch time by the various launch activities substantially masks any RF noise that might be generated by electrification of the vehicle itself.

## RADIOMETRIC MEASUREMENT OF THE APOLLO VEHICLE EXHAUST TEMPERATURE<sup>a</sup>

### Purpose

After the Apollo 12 vehicle was struck by lightning, a calculation was made of the vehicle exhaust breakdown electric field strength as a function of height above ground (ref. 2). A semiempirical exhaust temperature profile was used in the exhaust breakdown electric field strength calculation. To confirm this temperature profile, a radiometric measurement of the exhaust temperature of the Apollo 14 vehicle was performed.

### Experiment Configuration

A two-channel infrared radiometer was used to measure radiant emission from the exhaust plume in two narrow spectral bands centered at 1.68 and 1.26 microns. The radiometer was installed at a location 5 miles west of the launch pad (fig. 3) at a height approximately 20 feet above the ground, and was held stationary while the vehicle passed through the field-of-view. The radiometer was modified from its normal configuration such

<sup>a</sup>Data included in this section were extracted from a report submitted by C. A. Morgan and R. C. Baldwin of the Lockheed Electronic Company.



that the field of view was changed from  $10^\circ$  circular to rectangular by placing a slit at the field stop which measured 0.002 inch vertically by 0.20 inch horizontally. The field-of-view was approximately 100 feet in the vertical direction by 1000 feet in the horizontal direction, and was centered 400 feet above the top of the Apollo 14 vehicle. Temperature was determined from a ratio of Planck's equation at two wavelengths (ref. 3). Two lead sulfide detectors were used in the a-c photo-conductive mode and their outputs were amplified approximately 1000 times with three stages of amplification. Mechanical chopping of both light beams was used to modulate the radiation falling on the detectors.

A 14-track analog tape recorder was used to store the radiometer output in the field. Standard time code signals (IRIG B) were also recorded. In the laboratory, the recorded radiometer signals were played through a peak detector and displayed by a strip chart recorder calibrated 0 to 5 volts and 0 to 2.5 volts, peak-to-peak, as a function of time.

#### Data

Acquisition of signal occurred as the base of the Saturn V passed through the field-of-view, resulting in the signal voltages shown in figure 12. The peak signal voltages of both channels, which were within the nominal operating limits of the electronics, were 5.1 volts for the 1.26-micron channel and 4.3 volts for the 1.68-micron channel.

Using the calculation technique described in reference 3, the temperature time profile of figure 13 was computed. The peak temperature was  $2560^\circ\text{K}$ . The exhaust entered the field-of-view at a temperature of  $1480^\circ\text{K}$ . Within 2 seconds of entering the field-of-view, the temperature decreased until it was lower than the capability of the instrument to respond, approximately  $1000^\circ\text{K}$ .

In figure 13, the temperature is seen to decrease over the period of 14.1 seconds to 14.6 seconds after lift-off, just prior to the exhaust plume entering the field-of-view. One explanation for this phenomenon might be that the Saturn V ignition produced flames, hot gas, and hot dust particles which extended into the field-of-view and then dissipated, producing the observed temperature decrease.

Measurement precision as determined from gain-versus-voltage ratios with blackbody temperature as a parameter results in uncertainties of  $15^\circ\text{K}$  at  $1410^\circ\text{K}$ ,  $105^\circ\text{K}$  at  $1950^\circ\text{K}$  and  $250^\circ\text{K}$  at the nominal peak temperature of  $2560^\circ\text{K}$ .

\*Optical pyrometer measurements of peak plume temperature performed by Dr. E. Phillip Krider, University of Arizona, yielded a value of  $2440^\circ\text{K}$ .

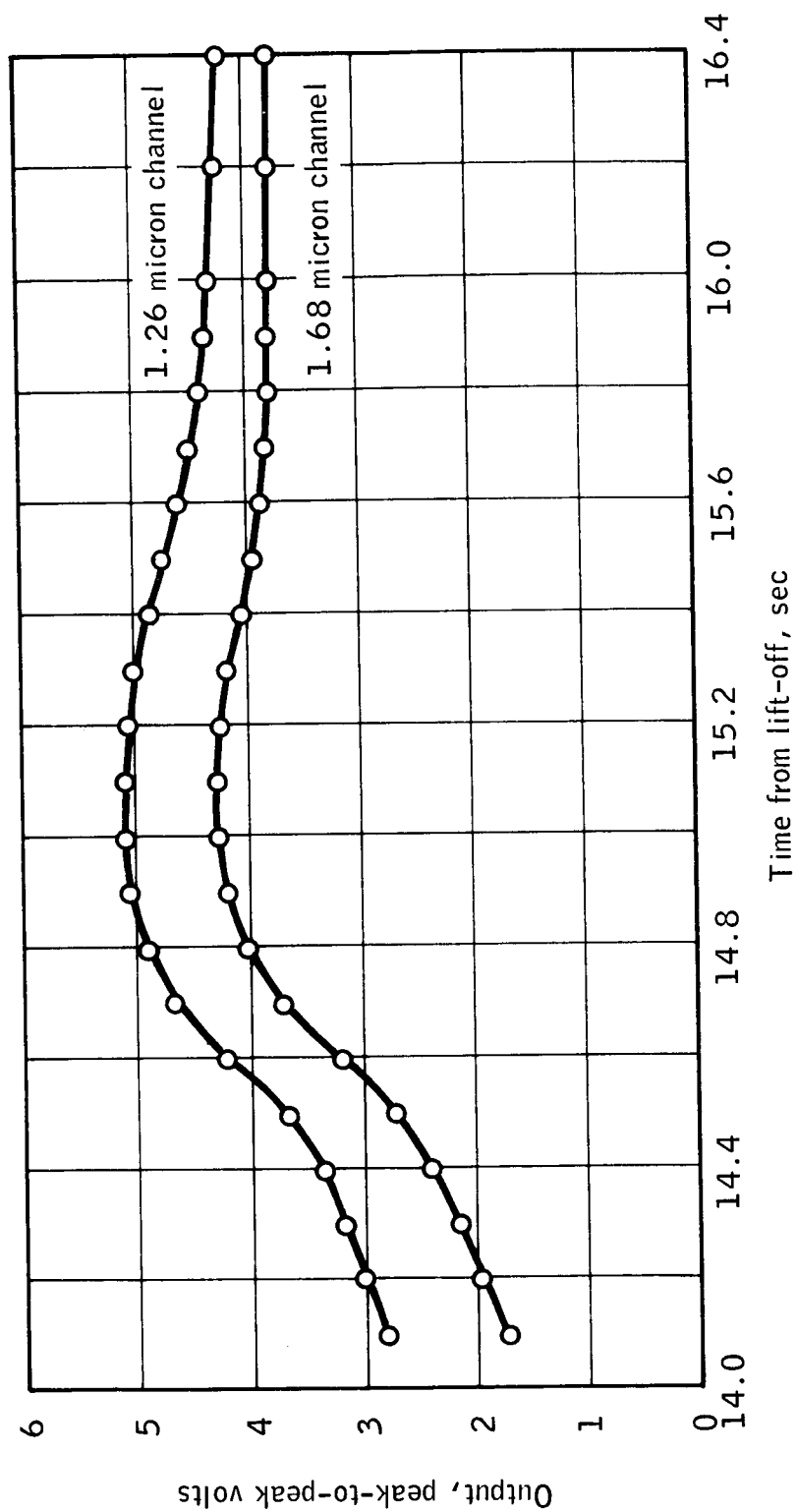


Figure 12.- Radiometer output as a function of time from lift-off.

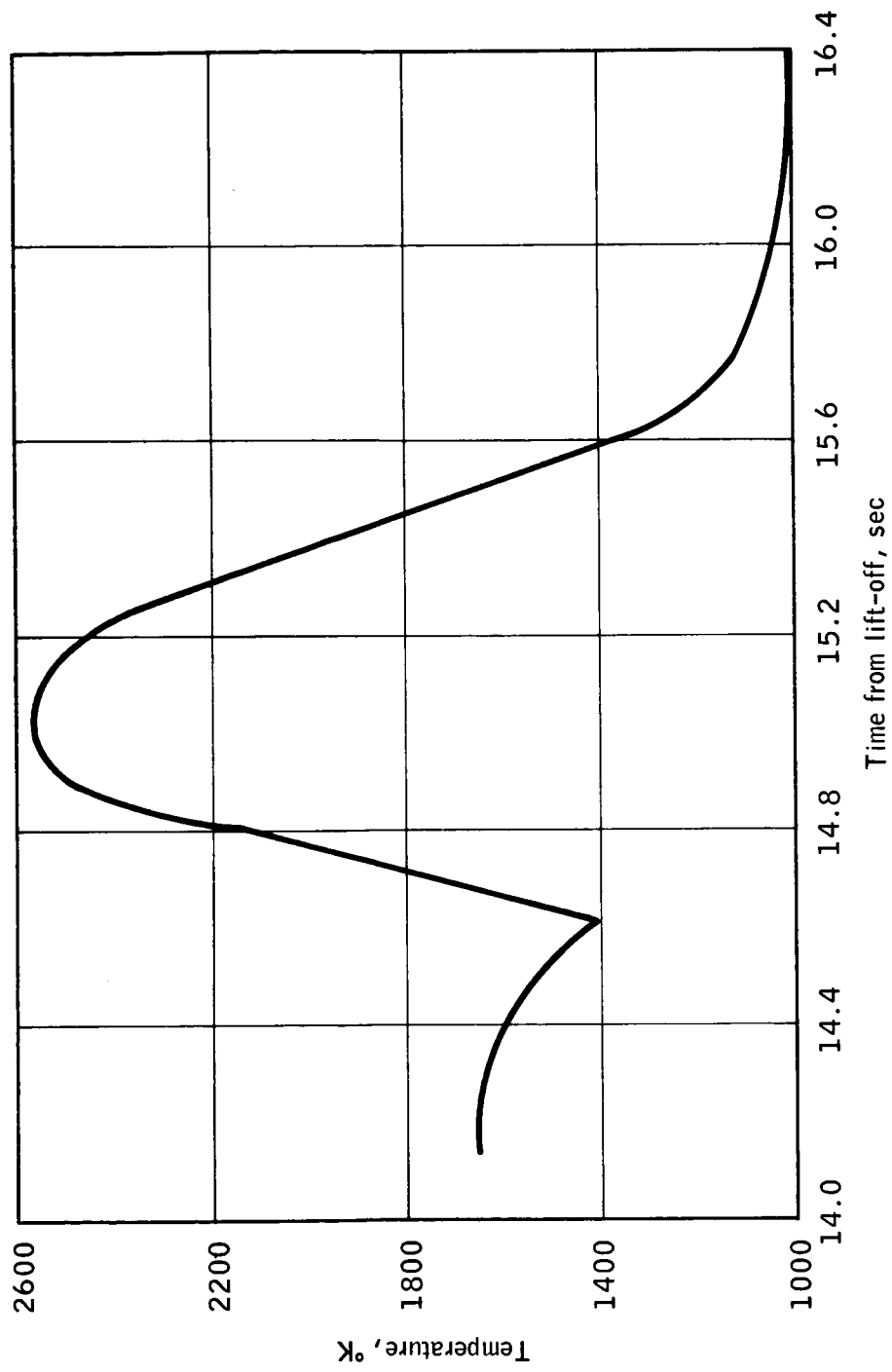


Figure 13.- Exhaust temperature as a function of time from lift-off.

## Analysis and Results

In figure 14, the infrared radiometer data are compared with Boeing Company measurements on a single F-1 engine and the semiempirical calculation of the temperature profile mentioned previously. The experiment data indicate that the temperature decay drops significantly as a function of distance behind the exit plane of the engines as compared to the calculated values which were based on the single F-1 engine data. There are a number of possibilities which might explain the differences: First, the Boeing Company data were obtained from a horizontal firing engine as compared to the vertical Saturn V launch. Second, perhaps the Boeing Company firing represented an exhaust with more carbon than was present during the Apollo 14 launch, with the result that the blackbody radiation did not extend as far down the Apollo 14 exhaust. Third, perhaps differences in measurement techniques and accuracies could account for the inconsistencies.

Calculated values of the probable upper and lower limits of the exhaust conductivity are shown in figure 15. These estimates were obtained using the temperature from figure 14 and the theoretical approach described in reference 2. The calculations show that the visible exhaust (which extends downward about 800 feet) is a relatively good conductor. For temperatures lower than about 400° K, there are negligible free electrons and hence the conductivity is due entirely to ions.

In the brightest part of the visible exhaust (which extends from 100 to 200 feet below the exhaust exit plane) the electron and ion densities are probably between  $10^8$  and  $10^{11}$  per cubic centimeter. Ion densities fall to about  $10^6$  per cubic centimeter at the bottom of the visible exhaust.

## MEASUREMENT OF LIGHTNING ELECTRIC FIELDS<sup>a</sup>

### Purpose

Measurements of radiation fields resulting from lightning strokes were made at the Kennedy Space Center in June and July of 1971 to acquire data from which peak lightning channel currents might be derived.

<sup>a</sup>Data included in this section were extracted from a report submitted by Martin A. Uman of Westinghouse Research Laboratories.

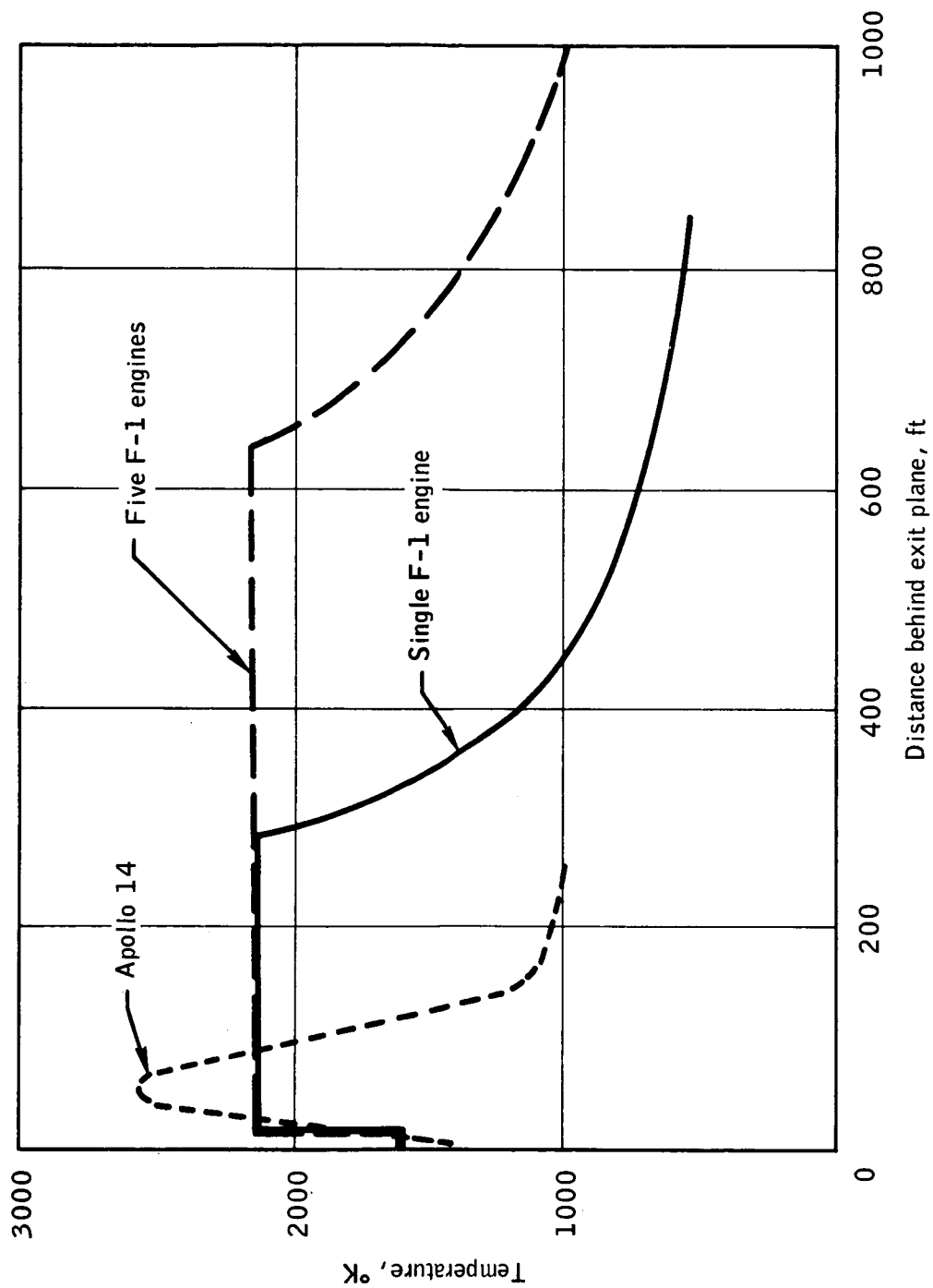
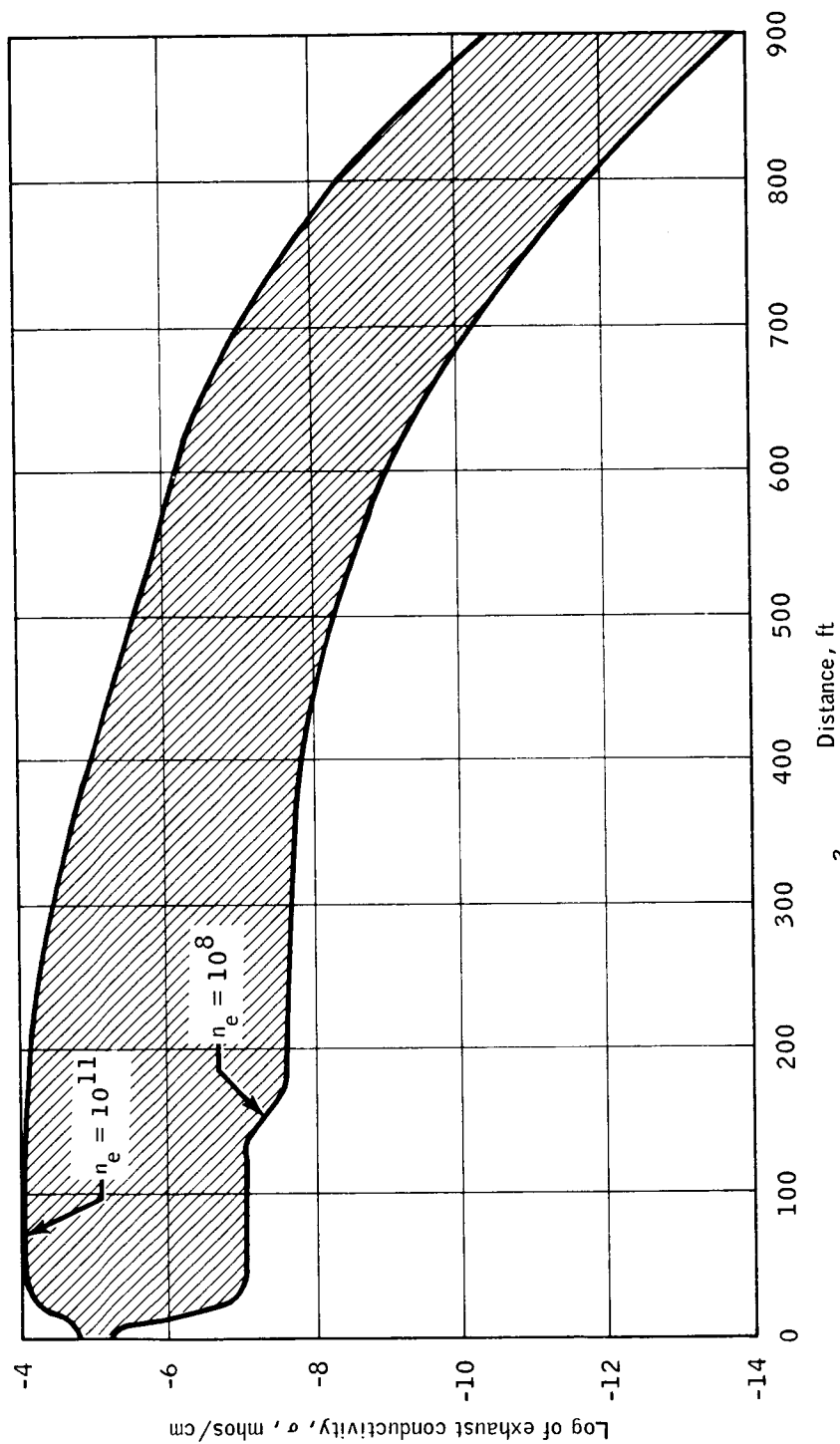


Figure 14.- Exhaust temperature characteristics.



Note:  $n_e$  represents electron and ion density per cm<sup>3</sup>

Figure 15.- Exhaust conductivity versus distance.

### Theory

Analytical techniques (ref. 4) have been developed which show how return stroke lightning currents can be obtained from the measured magnetic or radiation fields of lightning. By assuming that the lightning channel acts as a vertical transmission line and that radiation fields are being measured, the following expression relates peak channel current ( $I_p$ ) to peak electric field ( $E_p$ ).

$$I_p = \frac{16.5 D E_p c}{v} \text{ amperes}$$

where  $D$  is the distance in kilometers from the measurement point to the lightning,  $c$  is the speed of light ( $3 \times 10^8$  m/sec),  $v$  is the return stroke velocity in meters per second, and  $E_p$  is measured in volts per meter. Thus, to determine peak current,  $E_p$ ,  $D$  and  $v$  must be known.

For purposes of analysis, a maximum value for the return stroke velocity ( $v$ ) was assumed which results in the minimum value for current ( $I_p$ ). For first strokes in multiple-stroke flashes<sup>b</sup>, Schonland et al. (ref. 5) give a range for  $c/v$  of 1.5 to 10. Therefore, 1.5 was used in the analysis. For subsequent strokes in multiple stroke flashes, Schonland (ref. 6) gives a range of  $c/v$  of 2.7 to 12.5; therefore, 2.7 was used.

### Experiment Configuration

The electric field was measured with an antenna and recording system having an accuracy of  $\pm 15$  percent and a time resolution of 0.5 microsecond. The distance ( $D$ ) was determined by using thunder ranging which limited stroke distances to 15 kilometers and severely limited the number of accurate distance ranges obtained. Occasionally, an isolated distant storm was present making possible a moderately accurate lightning distance determination from radar weather data. Also, a few ranges were obtained photographically using two cameras separated by several kilometers.

### Data and Analysis

Electric field waveforms and good distance ranges were obtained for 164 strokes comprising 39 flashes. These data were taken on eight different days and represent lightning over both land and water. The flashes

<sup>b</sup> A complete lightning discharge, generally lasting 0.5 second, is called a flash. A flash is made up, on the average, of 3 or 4 intermittent discharges called strokes.

studied were between 1.1 and 32 kilometers in distance. The majority of the data (96 strokes comprising 18 flashes) were obtained on July 19, 1971. Lightning during the July 19 storm was between 1.1 and 10 kilometers distant. The storm was probably the most active for which data were taken.

Information on minimum values of peak current as computed from the preceding equation, using maximum stroke velocities, is shown in figure 16. Also indicated in figure 16 are the current rise-times (zero to peak) for the larger peak currents.

All currents over 60 kA in figure 16 were from the July 19 storm. The measured median peak current in that storm was 55 kA. All currents over 85 kA were due to subsequent strokes. The median of all data except that of July 19 was 16 kA. The median of all the data was 38 kA.

Two major measurement errors are such as to produce a minimum value of peak current. (1) If the channel is not vertical, the electric field measured will be smaller than if it is vertical (for the same channel current), and hence a smaller current than actual will be computed. This error should be less than 40 percent. (2) Thunder ranging generally results in a slight underestimation of the distance to the main current channel since sound is heard first from the nearest branches or in-cloud channels. This error becomes larger as the strokes come closer to the recording source. In the present data the error probably does not exceed 20 percent. The measuring system itself, as previously stated, is accurate to  $\pm 15$  percent.

The maximum return stroke velocities used were taken from data obtained in South Africa and represent the maximum of 14 first strokes and an unstated number of subsequent strokes. It is not likely that return stroke velocities in Florida are much different from those in South Africa, but it is a possible uncertainty. Return stroke velocities cannot exceed the speed of light. If, for example, subsequent-stroke return-stroke velocities were equal to the speed of light, then all the peak currents over 85 kA in figure 16 would be a factor of 2.7 less than shown.

The minimum peak currents presented should not be considered an adequate statistical sample in any sense, as the data sample is much too small.

### Results

Probably the most significant aspect of the present work is the identification of unusually large currents with very fast rise times. Five minimum peak currents have been measured between 140 and 160 kA. Since the maximum probable return stroke velocities were used, the chances are good that one or more of these currents, as well as some of the lower currents, were in the 200 to 400 kA range. The highest currents previously



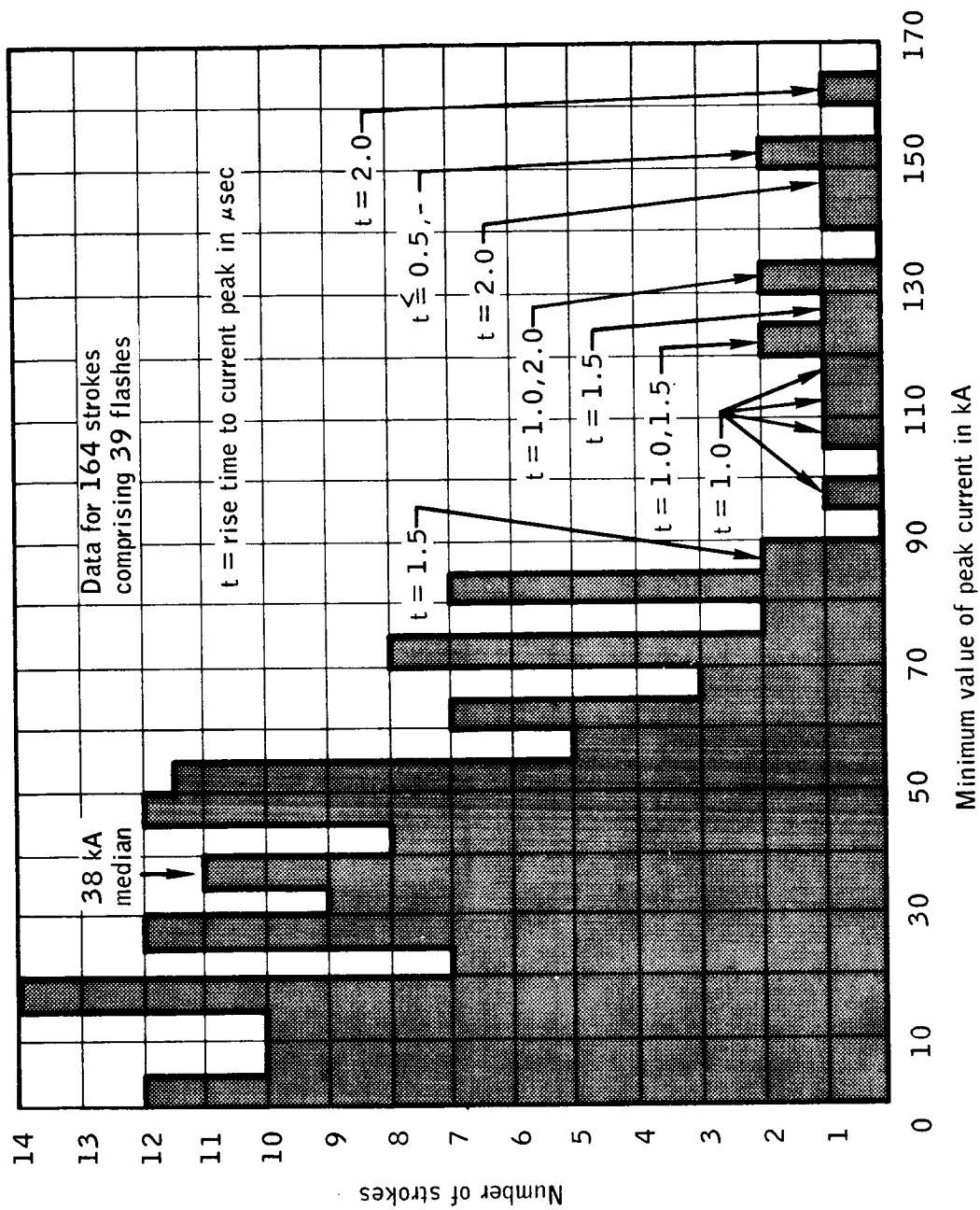


Figure 16.- Histogram of the number of lightning strokes having a given minimum value of peak current.

recorded anywhere in the world are near 200 kA (ref. 7). Further, a minimum value for the maximum current rate-of-rise (average from zero to peak) of about 300 kA/ $\mu$ sec (152 kA in less than 0.5  $\mu$ sec) was measured. The highest value of current rate-of-rise previously reported is 80 kA/ $\mu$ sec (ref. 8) and represents, not the average from zero to peak, but the maximum during the current rise to peak. This measurement was of the current produced by a stroke in a shunt on a tower top in Lugano, Switzerland.

### CONCLUSIONS

The intensities of the electric fields produced by the Apollo vehicle exhaust clouds are similar to those produced by active thunderstorms, but their extent is far less than those of naturally electrified clouds so that the electric energy stored in the exhaust clouds is appreciably less than that required for lightning to occur. It was estimated that no more than about  $10^5$  joules of electrical energy was stored in the clouds produced by Apollo 14. Elements of natural lightning usually release  $10^8$  joules or more. However, the electrification produced by the launch of Apollo vehicles is significant and could interact with naturally electrified clouds to cause a hazard such as that experienced on Apollo 12.

The Saturn V exhaust can be considered a good conductor for a distance beyond the engine exit plane for approximately 200 to 300 feet.

The measured electric fields of lightning strokes at the Kennedy Space Center indicate current rise rates as high as 300 kA/ $\mu$ sec with peak currents in excess of 160 kA.

REFERENCES

1. Pierce, E. T.: Waterfalls, Bathroom, and Perhaps, Supertanker Explosions.
2. Uman, M. A.: Electrical Breakdown in the Apollo 12/Saturn V First Stage Exhaust. 70-9C8-HIVOL-R1, Westinghouse Research Laboratories. May 4, 1970.
3. Morgan, C. A.; and Baldwin, R. C.: Radiometric Temperature Measurement of Apollo 14/Saturn V Exhaust. 649D.21.053, Lockheed Electronics Company/Houston Aerospace Systems Division. March 1971.
4. Uman, M. A.; and McLain, D. K.: Lightning Return Stroke Current from Magnetic and Radiation Field Measurements. J. Geophys. Res., vol. 75, 1970, pp. 5143-5147.
5. Schonland, B. F. J.; Molan, D. J.; and Collens, H.: Progressive Lightning. Proc. Roy. Soc. London, vol. A, no. 152, 1935, pp. 595-625.
6. Schonland, B. F. J.: The Lightning Discharge. Handb. Phys., vol. 22, 1956, pp. 576-628.
7. Uman, M. A.: Lightning. McGraw-Hill Book Co., Inc., 1969, pp. 114-137.
8. Berger, K.; and Vogelsanger, E.: Messungen und Resultate der Blitzforschung der Jahre 1955-1963 auf dem Monte San Salvatore. Bull. SEV, vol. 56, 1965, pp. 2-22.